EUROPEAN ORGANIZATION FOR NUCLEAR RESEARCH

CERN-EP/86-42
April 1st, 1986

The Bose-Einstein Correlations In Deep Inelastic μp Interactions at 280 GeV

The European Muon Collaboration

Aachen[1], CERN[2], DESY (Hamburg)[3], Freiburg[4], Hamburg (University)[5], Kiel[6], LAL (Orsay)[7], Lancaster[8], LAPP (Annecy)[9], Liverpool[10], Marseille[11], Mons[12], MPI (München)[13], Oxford[14], RAL (Chilton)[15], Sheffield[16], Torino[17], Uppsala[18], Warsaw[19] and Wuppertal[20].

M. Arneodo[17], A. Arvidson[18], J.J. Aubert[11], B. Badelek[19a)], J. Beaufays[2], C.P. Bee[8b)], C. Benchouk[11], G. Berghoff[1], I. Bird[8c)], D. Blum[7], E. Böhm[6], X. de Bouard[9], F.W. Brasse[3], H. Braun[20], C. Broll[9+)], S. Brown[10d)], H. Brück[20e)], H. Calen[18], J.S. Chima[15f)], J. Ciborowski[19a], R. Clifft[15], G. Coignet[9], F. Combley[16], J. Coughlan[8g)], G. D'Agostini[11], S. Dahlgren[18], F. Dengler[13], I. Derado[13], T. Dreyer[4], J. Drees[20], M. Düren[1], V. Eckardt[13], A. Edwards[20h)], M. Edwards[15], T. Ernst[4], G. Eszes[9i)], J. Favier[9], M.I. Ferrero[17], J. Figiel[5j)], W. Flauger[3], J. Foster[16k)], E. Gabathuler[10], J. Gajewski[5], R. Gamet[10], J. Gayler[3], N. Geddes[14l)], P. Grafström[18], F. Grard[12], J. Haas[4], E. Hagberg[18], F.J. Hasert[1m)], P. Hayman[10], P. Heusse[7], M. Jaffré[7], A. Jacholkowska[2], F. Janata[5], G. Jancso[9n)], A.S. Johnson[14o)], E.M. Kabuss[4], G. Kellner[2], V. Korbel[3], J. Krüger[20e)], S. Kullander[18], U. Landgraf[4], D. Lanske[1], J. Loken[14], K. Long[14p)], M. Maire[9], P. Malecki[13], A. Manz[13], S. Maselli[17n)], W. Mohr[4], F. Montanet[11], H.E. Montgomery[2q)], E. Nagy[9i)], J. Nassalski[19r)], P.R. Norton[15], F.G. Oakham[15s)], A.M. Osborne[2], C. Pascaud[7], B. Pawlik[13], P. Payre[11], C. Peroni[17], H. Peschel[20], H. Pessard[9], J. Pettingale[10], B. Pietrzyk[11], B. Pönsgen[5], M. Pötsch[20], P. Renton[14], P. Ribarics[9i)], K. Rith[4c)], E. Rondio[19a)], A. Sandacz[19r)], M. Scheer[1], A. Schlagböhmer[4], H. Schiemann[5], N. Schmitz[13], M. Schneegans[9], M. Sholz[1], T. Schröder[4], M. Schouten[13], K. Schultze[1], T. Sloan[8], H.E. Stier[4], M. Studt[5], G.N. Taylor[14], J.M. Thénard[9], J.C. Thompson[15], A. de la Torre[5t)], J. Toth[9i)], L. Urban[1], L. Urban[9i)], W. Wallucks[4], M. Whalley[16u)], S. Wheeler[16], W.S.C. Williams[14], S.J. Wimpenny[10p)], R. Windmolders[12], G. Wolf[13].

Abstract

The Bose-Einstein correlation has been observed for pions in deep inelastic μp interactions at 280 GeV. The importance of non-interference correlations in the sample of like charge pion pairs and in the sample used for reference is discussed. The pion emission region is found to be spherical with a radius of 0.46 - 0.84 fm and the chaos factor λ is 0.60 - 1.08.

(Submitted to Zeits. für Physik C)

For footnotes see next page.

Addresses

1) III. Physikalisches Inst. A, Physikzentrum, Aachen, Germany.
2) CERN, Geneva, Switzerland.
3) DESY, Hamburg, Germany.
4) Fakultät für Physik, Universität Freiburg, Germany.
5) II Institut für Experimentalphysik, Universität Hamburg, Germany.
6) II Institut für Kernphysik, Universität Kiel, Germany.
7) Laboratoire de l'Accélérateur Linéaire, Université de Paris-Sud, Orsay, France.
8) Department of Physics, University of Lancaster, England.
9) LAPP IN2P3, Annecy-le-Vieux, France.
10) Department of Physics, University of Liverpool, England.
11) Centre de Physique des Particules, Faculté des Sciences de Luminy, Marseille, France.
12) Faculté des Sciences, Université de L'Etat à Mons, Belgium.
13) Max-Planck-Institut für Physik und Astrophysik, München, Germany.
14) Nuclear Physics Laboratory, University of Oxford, England.
15) Rutherford and Appleton Laboratory, Chilton, Didcot, England.
16) Department of Physics, University of Sheffield, England.
17) Istituto di Fisica, Università di Torino, Italy.
18) Gustav Werners Institut, University of Uppsala, Sweden.
19) Physics Institute, University of Warsaw, and Institute for Nuclear Studies, Warsaw, Poland.
20) Fachbereich Physik, Universität Wuppertal, Germany.

a) University of Warsaw, Poland
b) Now at University of Liverpool, England
c) Now at MPI für Kernphysik, Heidelberg, Germany.
d) Now at TESA S.A., Renens, Switzerland.
e) Now at DESY, Hamburg, W. Germany.
f) Now at 30 Addison Ave., Hounslow, England.
g) Now at RAL, Chilton, Didcot, England.
h) Now at Jet, Joint Undertaking, Abingdon, England.
i) Now at Central Research Institute for Physics of the Hungarian Academy of Science, Budapest, Hungary.
j) Now at Institute of Nuclear Physics, Krakow, Poland.
k) Now at University of Manchester, England.
l) Now at British Telecom, London, England.
m) Now at Krupp Atlas Elektronic GmbH, Bremen, Germany.
n) Now at MPI, Munich, Germany.
o) Now at SLAC, Stanford, California.
p) Now at CERN, Geneva, Switzerland.
q) Now at FNAL, Batavia, Illinois, U.S.A.
r) Institute for Nuclear Studies, Warsaw, Poland.
s) Now at NCR, Ottawa, Canada.
t) Now at Universidad Nacional, Mar del Plata, Argentina.
u) Now at University of Durham, England.
+) Deceased

1. Introduction

This paper presents a study of the Bose-Einstein interference effect in like charge pions from 280 GeV deep inelastic muon-proton interactions. The symmetrisation of the wave function of two identical bosons can give rise to an observable interference pattern. The main feature of this pattern is the enhancement of boson pairs close in phase space. Its shape depends on the distribution of boson sources in space and time and on the degree of their coherence (see [1] for the theoretical review).

The first application of this effect was in astronomy, to measure the angular size of stellar objects [2]. Later it was re-discovered in pion spectra from $p\bar{p}$ annihilation [3] and established as a possible tool to analyse the space-time structure of the emission region of particles created in high energy interactions [4-8].

Since then measurements of the size of the pion emission region have been made in e^+e^- [9-12], hadron-hadron [13-15] and nucleus-nucleus [16] collisions giving a result of about 1 fm in the former two cases and up to several fermis in the latter (see ref. [17] for a review).

The pure interference pattern of two charged pions can be distorted by their mutual electromagnetic and strong interactions and also by other dynamical correlations present in the production. While the first two effects are important only at small relative velocities, the last is still not well known and requires careful study. There might be many sources of such correlations, e.g. resonance production [5], coherence effects [1,18], short range correlations induced by the fragmentation etc.

In this paper the first results on the Bose-Einstein (BE) correlations among like-sign charged pions from deep inelastic lepton-proton scattering are presented. As in e^+e^- interactions, the effects are related to the hadronisation resulting from the simple parton configuration with the advantage that the initial parton direction is better known.

The aim of this paper is

a) to isolate the interference effect from other correlations which are present in hadronic production or are due to the construction of the non-interfering (reference) sample,

b) to study the shape of the pion source.

In this study we assume that the non-interference correlations are reproduced by the Lund model [19] and that they factorise in the overall effect. It should be noted that the Lund model, with suitably chosen parameters, successfully reproduces many aspects of hadron production in our data [20,21,22].

2. Parameterisation of the Interference Effect

The most common parameterisation of the BE effect is in terms of $\Delta p = p_i - p_j$, the difference of the four momenta of two like sign pions. This can be further split into $\vec{\Delta p} = \vec{p}_i - \vec{p}_j$ and $|\Delta E| = |E_i - E_j|$ dependences which probe separately the spatial and the life time distributions of the pion sources. If the space and life time distributions are independent the coincidence rate for like sign pion pairs is

$$I = 1 + f_1(\vec{\Delta p})\ f_2(|\Delta E|), \qquad (2.1)$$

where f_1 and f_2 are the Fourier transforms of the assumed source distribution functions $F_1(\vec{r})$ and $F_2(t)$ respectively. Experimentally I is taken to be proportional to the ratio of like sign pion pairs to pairs from a reference sample which are assumed to be free from the interference effect.

Two different kinds of functions F_1 and F_2 have been proposed in the literature and were used in previous analyses.

For $F_1(\vec{r})$:

i) a uniform distribution of sources on a disk of radius R [4] oriented such that the normal to the disk direction is along $\vec{n}=(\vec{p}_i+\vec{p}_j)/|\vec{p}_i+\vec{p}_j|$, gives

$$f_1 = 4\, J_1^2(q_t R)/(q_t R)^2 \tag{2.2}$$

where $\vec{q}_t=\vec{n}\times\Delta\vec{p}$ measures the source size in the direction of $\vec{n}$ and J_1 is the first order Bessel function,

ii) a Gaussian distribution of sources on the ellipsoid whose major axis is oriented in the direction of the initial collision gives

$$f_1 = e^{-\Delta p_{\parallel}^2 R_{\parallel}^2 \; - \; \Delta p_T^2 R_T^2} \tag{2.3}$$

where $R_{\parallel(T)}$ are the rms values of the Gaussian distributions along and perpendicular to the collision axis (i.e. the virtual photon direction) and $\Delta p_{\parallel(T)}$ are the corresponding projections of $\Delta\vec{p}$.

For $F_2(t)$:

i) an exponential decay function with a life time τ gives

$$f_2 = [1 + (\Delta E\tau)^2]^{-1} \ , \tag{2.4}$$

ii) a Gaussian decay function with rms value of τ gives

$$f_2 = e^{-(\Delta E\tau)^2} \tag{2.5}$$

There is no physical justification to prefer either of these two parameterisations of F_1 or F_2. However, the values of R and τ have different meaning for the two parameterisations and fits to the data can

therefore give different results. In particular the parameterisations involving (2.2) and (2.4) have been proposed by Kopylov and Podgoretski [4] and have often been used in the analysis of data. It should also be noted that the above description of the effect is not Lorentz-invariant [6,23]. The variables calculated in the CMS of the initial collision are generally used.

In practice a simultaneous fit to f_1 and f_2 would require high statistics and careful handling of the correlations between the variables $(\Delta\vec{p}^2)$ and (ΔE^2). Therefore an alternative, and Lorentz invariant, form of the parameterisation for I is used here [9]:

$$I = 1 + e^{-\tilde{M}^2 R^2} , \qquad (2.6)$$

where $\tilde{M}^2 = -(\Delta p)^2 = M^2 - 4m_\pi^2$ and M is the invariant mass of the pion pair. This parameterisation becomes identical to that given by (2.3), which has clear physical interpretation, in a system where $\tilde{M}^2 = (\Delta\vec{p})^2$, i.e. $\Delta E = 0$. Therefore the parameter R given by (2.6) can be interpreted as the rms size of the pion sources as seen from the CMS of the pion pairs (where $\Delta E = 0$).

It has been noticed [18] (see also [1]) that the functional form (2.1) implies complete chaos of the pion sources, which need not be the case. For a given degree of chaos, λ ($0 \leq \lambda \leq 1$), one would expect $I = 1 + \lambda f_1 f_2$. There are also other dynamic sources which can lead to a value of $\lambda < 1$ [5]. It is important to notice that experimental biases can lead to a considerable decrease of the parameter λ (see sect. 3).

In our analysis we use mostly the following parameterisation:

$$I = 1 + \lambda e^{-\tilde{M}^2 R^2} \qquad (2.7)$$

which has also been adopted in the analysis of the BE effect in e^+e^- interactions [9-11]. The energy and momentum variables used in the analysis are calculated in the CM of the produced hadronic system.

3. Data Selection and Corrections

The data were taken in the M2 muon beam at CERN at an incident muon energy of 280 GeV using the EMC (NA9) apparatus which consisted of a double magnetic spectrometer. The vertex spectrometer (VS) contained a 1 metre long liquid hydrogen target placed inside a streamer chamber. The scattered muon and fast forward hadrons enter the forward spectrometer magnet (having a bending sense opposite to the VS magnet) where the tracks (FS tracks) were detected and measured in an arrangement of proportional and drift chambers. Low momentum tracks were detected and measured in the streamer chamber (SC tracks) whilst intermediate momentum tracks were detected and measured in the streamer chamber and a system of proportional chambers and drift chambers positioned to detect tracks with a large bending angle. This apparatus gave almost complete acceptance for the detection of final state hadrons over the full solid angle and for momenta greater than 200 MeV/c, giving essentially 4π coverage in the centre of mass frame.

An extensive particle identification system was used. This consisted of a set of gas Cerenkov counters, filled with neopentane and nitrogen for identification of hadrons with low and intermediate momenta, aerogel Cerenkov counters and a time of flight hodoscope system for low momenta and a large Cerenkov counter filled with neon for fast forward particles. The apparatus, identification and analysis procedures are extensively described elsewhere [24].

In order to keep radiative corrections below 20% and also to have good resolution and acceptance, the following kinematic cuts were used:

$$Q^2>4\ \mathrm{GeV}^2,\ 4<W<20\ \mathrm{GeV},\ 20<\nu<260\ \mathrm{GeV},\ \nu<0.9\ E_{beam},\ \theta_\mu'>0.75^\circ$$

where $-Q^2$ is the square of the four-momentum transferred between the incident and outgoing muons, W is the total CM energy of the final state hadrons, ν and Θ_μ' are the energy transferred between the incident and scattered muons and the scattering angle in the laboratory system, respectively.

The charged hadrons were selected if they gave an acceptable fit to the primary vertex (not visible in the SC) which also included the beam and the scattered muon. Those tracks consistent with a V^o vertex or with only secondary vertices were eliminated. In order to reduce a possible background imitating the BE effect and arising from the double counting of tracks in the SC and FS systems only tracks measured in the SC were kept. These tracks constitute about 84% of the total multiplicity and the SC acceptance covers all except the most forward region of $x_F(x_F \gtrsim 0.2)$. A sample of pairs of tracks with small relative momentum was examined on the scanning table and the double counting among such SC tracks was found to be negligible. The momentum resolution for tracks measured in the SC varies from 1% at 1 GeV to 20% at 20 GeV. Only tracks with momentum resolution of better than 20% were kept.

In the selected sample about 50% of the hadrons were identified. The Lund model [19] predicts the following composition of hadrons in this sample: $\pi^{\pm}/K^{\pm}/(p+\bar{p})=80/9/11$. In the momentum regions where particles can be fully identified the predictions of the Lund model are compatible with the data [22]. All unidentified hadrons of negative charge were assumed to be pions. There is a large fraction of protons in the target fragmentation region among the positive particles. A Monte Carlo study made on the basis of the Lund model indicates that in the region $x_F(\pi)<-0.2$ and at the same time $x_F(p)>-0.9$, about 80% of such hadrons are protons. Therefore a non-identified positive hadron was taken as a pion only if $x_F(\pi)>-0.2$ or if $x_F(p)<-0.9$ [25]. Here $x_F(h) = 2*p_{||}^{CMS}(h)/W$ where $p_{||}^{CMS}$ is calculated using the mass of hadron (h).

Only pions were used in the analysis and the events were required to have at least 3 charged pions with at least one pair of opposite charges. The final sample consisted of 17343 events with 60000 (π^+,π^+), 38300 (π^-,π^-) and 126000 (π^+,π^-) track combinations.

All the hadronic distributions which are discussed below were corrected for acceptance and radiative effects in each bin in the following way: firstly, a sample of events was generated according to the Lund model [19], including internal bremstrahlung photons. Each event was then fully simulated in the EMC-NA9 apparatus taking into account the secondary hadron interactions, V^o decays and photon conversions. The simulated hits in all detectors were then passed through the pattern recognition programs used for the data and included the effects of the apparatus acceptance, detector efficiencies and measurement errors. The signals from the Cerenkov counters and the SC film measurements were also simulated. The simulated events were processed through the same chain of the reconstruction and fitting programs as used for data. The correction factor, for a given data distribution, is taken as the ratio of the corresponding distributions, per interacting muon, from the simulated and the generated samples. The unbiased experimental distributions were obtained by dividing each measured distribution by the corresponding correction factor. Figure 1 shows the correction factor as a function of $\tilde{M}^2$ for (π^+,π^+) and (π^-,π^-) combinations. At small values of $\tilde{M}^2$ the overall correction factor is larger than one due mostly to the misidentification of pions, to the admixture of tracks from decays and to secondary interactions of hadrons close to the primary vertex which survived the cuts applied to exclude them. It should be noted that in taking track combinations the correction factors are enhanced by about a factor of two relative to those for single particle distributions.

The effects of track misidentification and of wrong track associations with the main vertex on the values of λ obtained by fitting the formula (2.7) were investigated in detail, using the sample of events generated and simulated in the apparatus. Each simulated track was checked to see that it came from the main vertex and that it had been correctly identified. The ratio of the unbiased simulated sample (containing only well identified tracks from the main vertex) to the total simulated sample (representing the data) was studied as a function of $\tilde{M}^2$ for the like-charge combinations. This ratio was independent of $\tilde{M}^2$ with a value of 0.48. This represents a factor (C_λ) which relates the true value of λ to that measured in the data: $\lambda_{true}=\lambda_{measured}/0.48$. Such effects were found not to alter the value of R.

4. Results

4.1 Extraction of the Bose-Einstein Effect

The BE effect is searched for in the $\tilde{M}^2$ distribution for like sign (LIKE) pion combinations. The $\tilde{M}^2$ distributions for (π^+,π^+) and (π^-,π^-) combinations were found to be identical within the errors and in the subsequent analysis the sum of these is used.

In order to extract the BE effect from the LIKE sample a reference (REF) $\tilde{M}^2$ distribution has to be constructed. The pairs of tracks in the REF sample should not be subject to the interference effects but should contain the same kinematic and dynamic correlations as the LIKE sample. The practical realisation of the first requirement is simple. In addition the kinematic correlations, due to energy and momentum conservation, can be reproduced to a good approximation. The most difficult to imitate are the dynamic correlations. In order to study these the $\tilde{M}^2$ dependence of the LIKE/REF ratio are presented using three different commonly used reference samples where each is corrected with a separately determined correction factor (see sect.3):

- REF (1): (π^+,π^-) combinations from the same event.

- REF (2): (π^+,π^-) combinations of pions with random p_T from the same event. For each π the momentum is calculated in the CM of the produced hadronic system and it is decomposed into $p_{||}$ and $\vec{p}_T$ relative to the virtual photon direction. Its charge and $p_{||}$ are kept unchanged but $\vec{p}_T$ is chosen at random from one of the other pions in the event.

- REF (3): LIKE combinations using events with random tracks. The events are split into three classes according to W: $4 < W \leq 10$ GeV, $10 < W \leq 15$ GeV and $15 < W \leq 20$ GeV. For each event a reference event having the same number of positive and negative pions was constructed. Each track of the reference event was selected at random and from a different event belonging to the same class.

The LIKE/REF ratios obtained with different reference samples are shown in fig. 2a. Although a rise at small $\tilde{M}^2$ is seen for each of the reference samples there is lack of consistency in the overall normalisation and the shape of the effect. The shape dependent parameters R and λ are extracted by fitting the following function to the ratios:

$$F(R,\lambda,\delta,N;\ \tilde{M}^2) = N\ (1 + \lambda e^{-\tilde{M}^2R^2})\ (1 + \tilde{M}^2\delta) \qquad (4.1)$$

where δ takes into account the slow rise of the ratios at large values of $\tilde{M}^2$ and the fit is made in the $\tilde{M}^2$ range from 0 to 2 GeV^2. For the sample REF (1) we exclude from the fit the $\tilde{M}^2$ range from 0.38 GeV^2 to 0.58 GeV^2 where the contribution from the ρ^o is strong. The following shape parameters are obtained: R_1=1.30 ± 0.84 fm and λ_1=1.00 ± 0.17, R_2=0.47 ± 0.12 fm and λ_2=0.69 ± 0.08, R_3=0.55 ± 0.03 fm and λ_3=1.19 ± 0.06, where the λ values have been corrected with the factor C_λ (see sect. 3) and the parameter δ is in the range 0.08-0.2.

For each reference sample we check the consistency of the non-interfering kinematic and dynamic correlations, in the $\tilde{M}^2$ distributions, between the LIKE and REF samples. This check is made using the Lund model which does not contain interference effects [19] where the generated events were subjected to the same kinematic cuts as the data. The comparison of the LIKE and REF samples is shown in fig. 2b. For each of the reference samples the residual dynamic and/or kinematic correlations are seen to be different from those in the LIKE sample. The sizeable differences at small $\tilde{M}^2$ affect the shape of the BE effect obtained from the data. In the case of REF (1) the differences are seen throughout the whole $\tilde{M}^2$ range and they are due to the two and three body decays of resonances. This is illustrated in fig. 3 which summarises the effects of resonance contributions to the LIKE and REF 1 samples. With the ratio of pseudo-scalar to vector meson production set to one the following observation can be made:

1. For the directly produced pions (not from resonance decays), the ratio LIKE/REF (1) is a flat, smoothly varying function of $\tilde{M}^2$, as expected from the model which does not contain the interference effects.

2. In the sample REF (1) at small $\tilde{M}^2$ the contribution from η, η' and ω decays varies strongly with $\tilde{M}^2$ and reaches 30% of all $(\pi^+\pi^-)$ combinations.

3. In the LIKE sample the contribution from η' decays reaches 16% at threshold.

The differences between the LIKE and REF (2) or REF (3) show that the reference sample depends on the method used for randomisation.

In the following analysis we assume that the correlations seen in fig. 2b from the Lund model are also present in the data (fig. 2a) and that they factorise from the BE effect. Hence in the extraction of the BE effect we divide the ratio LIKE/REF for the data by the corresponding ratio from the Lund model. The results are shown in fig. 2c. In spite of the differences seen separately for the data and the Lund model, these ratios show a trend which is similar for each reference sample in both shape and absolute magnitude. The approximate independence of these results from the REF sample indicates that the method of extracting the BE effect is justified, i.e. that the BE effect approximately factorises from the other correlations which are in the Lund model.

The results of the fit of the parameterisation (4.1) to the double ratio of the data and the Lund prediction in fig. 2c are given in table 1. As expected these results differ from the results obtained from the ratio for the data alone. It is also seen that the results of the fit still depend on the reference sample. These differences can be taken to represent the residual uncertainties in extracting the BE effect due to the definition of the reference sample.

4.2 Background Studies

The results based on REF (1) are sensitive to the amount of resonance production assumed in the Lund model. For further discussion we choose REF (3) which is the most randomised sample. However, it should be noted that we still rely on the Lund model to correct for the differences in the non-interference correlations in the LIKE and REF (3) samples. In particular, we correct for the η' signal expected in the LIKE sample at small $\tilde{M}^2$.

The following checks were made on the results obtained with REF (3):

1. The same analysis was made using uniquely identified $\pi^{\pm}$ only. For this purpose both the SC and the FS tracks were used, since the double counting of tracks is unlikely in this case. The factor C_λ was determined to be 0.61 and the results were consistent with those obtained before.

2. Using uniquely identified $\pi^{\pm}$, $K^{\pm}$, p and $\bar{p}$ we have checked if the BE effect is absent in the ratio of

$$[(\pi,K)+(\pi,p)+(K,p)]_{\text{same sign}}/[(\pi,K)+(\pi,p)+(K,p)]_{\text{opposite sign}}$$

The results are inconclusive due to the large statistical uncertainties but are compatible with no effect.

3. Using the simulated events (see section 3) we have checked whether the BE effect is due to particle misidentification and backgrounds contributing to the small $\tilde{M}^2$ region only. The following sources of possible biases have been considered : η' decay, $\Delta^{++}\to p\pi^+$ with a proton identified as a π^+ and $K^{*\pm}\to K^o\pi^{\pm}$ with the K^o decay vertex taken at the primary interaction point. The results indicate that for both the LIKE and the REF (3) samples this leads to about 12% enhancement at small $\tilde{M}^2$ relative to the corresponding unbiased samples. However, this enhancement cancels out in the ratio LIKE/REF (3).

These checks clearly indicate that the enchancement at small $\tilde{M}^2$ in fig. 2c cannot be explained by contamination or background effects only.

We have also checked that the coulomb interactions within pairs of LIKE pions do not modify significantly the $\tilde{M}^2$ distribution for which the Gamov factor [26] was found to vary less than 1.5%.

The experimental resolution in $\tilde{M}^2$ has been estimated from the observed width of the K^o, $\sigma(\tilde{M}^2) = 0.025$ GeV^2, and the smearing correction to the fitted values of R is below 1%.

4.3 Results the Shape of the Emission Region

The results on the possible $|\Delta E|$ - dependence of the effect (see sect. 2) are presented in fig. 4 and table 1. The results for all pion pairs and for those with $|\Delta E|<0.2$ GeV are identical indicating that the contribution from larger values of $|\Delta E|$ does not modify the effect.

The shape parameters of the BE effect derived from the overall $\tilde{M}^2$ distribution (fig. 2c and table 1) refer to the region of pion sources averaged over all directions. However, it is possible that the emission region is highly non-spherical as postulated for example by the colour string models [26,27] where the string is oriented in the virtual photon direction and π mesons are emitted over its full length. An estimate of the longitudinal and the transverse sizes of the string can be made by selecting pion pairs for which the vector $\vec{\Delta p}$ makes an angle smaller or bigger than 45^o relative to the virtual photon line. The results are shown in fig. 5 and table 1. Within the errors there is no evidence for a significant departure from a spherical shape.

In a more rigorous approach, instead of using the variable $\tilde{M}^2$, one should investigate the $\Delta p_{\parallel}^2$ and Δp_T^2 dependence of the effect (see sect. 2).

Pion pairs were selected from two orthogonal bands in the ($\Delta p_{\parallel}$, Δp_T) plane; between $\Delta p^2_{T(\parallel)}$=0 and $\Delta p^2_{T(\parallel)}$=0.04 GeV^2. The ratio of LIKE/REF (3) from the data divided by the same ratio obtained from the Lund model is plotted in fig. 6 as a function of Δp^2_T or $\Delta p^2_{\parallel}$. The broken line in fig. 6 shows the effect expected from the spherical region as determined from the overall $\tilde{M}^2$ dependence. The Δp^2_T dependence is in agreement with the values obtained for all pions while the results on the $\Delta p^2_{\parallel}$ dependence are inconclusive due to the large statistical errors.

Comparing our results with those of e^+e^- studies reporting on the BE effect, we observe that the MARK II data [9] from the J/ψ region were not corrected for the possible differences in non-interference correlations between the LIKE and the REF (1) samples which were found to be important in the present analysis. In a similar analysis of the TASSO data [10] at 34 GeV to that presented here, the LIKE/REF (1) ratio was normalised using the Lund model and the value of λ corrected for background. Their λ value is smaller than ours (λ = 0.60 ± 0.09) while R is the same (R = 0.76 ± 0.12). In the analysis of the PEP-4 TPC data [11] at 29 GeV an iterative procedure was used to construct the REF (3) sample and its consistency with the LIKE sample was investigated using the Lund model. Their value of λ was corrected for background (λ=0.61±0.05±0.06) and is consistent with our value while the value of R is somewhat bigger (R = 0.65 ± 0.04 ± 0.05). Their results were also consistent with the shape of the interaction region being spherical. The data from the CLEO collaboration [12] was taken at an energy of 10.5 GeV. The LIKE/REF (1) ratio was not normalised with a model and gave the value of R at 0.85 ± 0.15 fm and the value of λ, corrected for long-lived particle decays, was 1.45 ± 0.25, both consistent with our results. In their experiment the LIKE/REF (2) ratio gave the same values of the shape parameters.

The above comparison shows approximate consistency of the results from e^+e^- and deep inelastic interactions. The remaining differences may be due to the residual non-interference correlations and to the systematic effects due to backgrounds in the analysed samples.

5. Conclusions

The Bose-Einstein interference effect has been studied in the $\tilde{M}^2$ distributions for pairs of like-sign pions relative to three different reference samples. The Lund model, which does not contain the Bose-Einstein effect, was used to study the correlations which affect the determination of the pion source parameters. We assume that the Lund model correctly describes such effects and that these factorise from the Bose-Einstein correlations. With these assumptions the interference effect can be extracted by taking the ratio of like sign pions to a reference sample from the data and dividing it by the same ratio from the Lund model. A similar boson interference effect was observed for all three reference samples.

The results are consistent with a spherical shape for the pion emission region with a radius of 0.46 - 0.84 fm and the supression factor λ of 0.60 - 1.08, depending on the reference sample.

The small longitudinal dimensions of the pion emission region observed here and the large longitudinal distances needed for jet formation as suggested by the EMC data on nuclear hadroproduction [27] and expected from models [28] (see also references in [27]) may indicate a space-time ordering of the hadron momenta within a jet. Such an ordering exists in the Lund model. If this is the case then bosons which interfere, i.e. the bosons which are close in phase space can only be found at nearby points in space and time. This ordering may also induce some coherence and lead to a λ value smaller than one [29].

References

1. M. Gyulassy et al., Phys. Rev. C20 (1979) 2267.
2. R. Hanbury Brown and R.Q. Twiss, Phil. Mag. 45 (1954) 663;
   Nature 178 (1956) 1046; 178 (1956) 1447.
3. G. Goldhaber et al., Phys. Rev. 120 (1960) 300.
4. G.I. Kopylov and M.I. Podgoretski, Sov. J. Nucl. Phys. 15 (1972) 219;
   18 (1973) 336; 19 (1974) 215;
   G.I. Kopylov, Phys. Lett. 50B (1974) 472.
5. R. Lednicky and M.I. Podgoretski, Sov. J. Nucl. Phys. 30 (1979) 432.
6. M.I. Podgoretski, Sov. J. Nucl. Phys. 37 (1983) 272.
7. E.V. Shuryak, Phys. Lett. 44B (1973) 387.
8. G. Cocconi, Phys. Lett. 49B (1974) 459.
9. G. Goldhaber, LBL report, LBL-13291 (1981)and Proceedings Int. Conf.
   on High Energy Physics, Lisbon 1981, p.767.
10. M. Althoff et al., DESY report, DESY 85-126, 1985;
    M. Althoff et al., Z. Phys. C29 (1985) 347.
11. H. Aihara et al., Phys. Rev. D31 (1985) 996.
12. P. Avery et al., Cornell report, CLNS-85/645.
13. M. Deutschmann et al., Nucl. Phys. 204B (1982) 333;
    CERN report CERN-EP/PH 78-1 (1978).
14. T. Akesson et al., Phys. Lett. 129B (1983) 269;
    Phys. Lett. 155B (1985) 128.
    A. Breakstone et al., Phys. Lett. 162B (1985) 700.
15. R. Carlsson et al., Phys. Scripta 31 (1985) 21.
16. S.Y. Fung et al., Phys. Rev. Lett. 41 (1978) 1592.
    J.J. Lu et al., Phys. Rev. Lett. 46 (1981) 898.
    W.A. Zajc et al., Phys. Rev. 29C (1983) 2173.
    D. Beavis et al., Phys. Rev. 27C (1984) 910.
17. G. Goldhaber, LBL report, LBL-19417 (1985).
18. G.N. Fowler and R.M. Weiner, Phys. Lett. 70B (1977) 201.
    A. Giovannini and G. Veneziano, Nucl. Phys. B130 (1977) 61;
    M. Biyajima, Phys. Lett. 92B (1980) 193.
19. G. Ingelman et al., Nucl. Phys. B206 (1982) 239.

20. EMC, M. Arneodo et al., Phys. Lett. 145B (1984) 156.
21. EMC, M. Arneodo et al., Phys. Lett. 149B (1984) 415.
22. EMC, M. Arneodo et al., Phys. Lett. 150B (1985) 458.
23. F.B. Yano and S.E. Koonin, Phys. Lett. 78B (1978) 556.
24. EMC, J.P. Albanese et al., Nucl. Instr. and Meth. 212 (1983) 111.
25. EMC, J.P. Albanese et al., Phys. Lett. 144B (1984) 302.
A.S. Johnson, Ph.D. Thesis, Nuclear Physics Laboratory, Oxford, HEP T 119 (1984).
26. L.I. Schiff, Quantum Mechanics, ed. McGraw-Hill, 1968.
27. EMC, A. Arvidson et al., Nucl. Phys. B246 (1984) 381.
28. B. Andersson et al., Phys. Rep. 97 (1983) 31.
29. M. G. Bowler, Z. Phys. C29 (1985) 617.

Table 1

Parameters R and λ obtained from fitting the ratio $[\frac{\text{LIKE}}{\text{REF (i)}}]_{\text{DATA}}/[\frac{\text{LIKE}}{\text{REF (i)}}]_{\text{LUND}}$ with the function (4.1) in $\tilde{M}^2$ range from 0 to 2 GeV^2.

Reference Sample	$\tilde{M}^2$ Distribution	R (fm)	$\lambda^{*)}$	χ^2 (NDF=12)
REF (1)	all $\tilde{M}^2$	0.84 ± 0.03 +)	1.08 ± 0.10 +)	12.4
REF (2)	all $\tilde{M}^2$	0.66 ± 0.01	0.60 ± 0.06	12.2
REF (3)	all $\tilde{M}^2$	0.46 ± 0.03	0.73 ± 0.06	20.3
REF (3)	for $\lvert\Delta E\rvert<0.2$ GeV	0.42 ± 0.06	0.71 ± 0.17	21.8
REF (3)	for $\lvert\Delta P_T\rvert>\lvert\Delta p_{\parallel}\rvert$	0.52 ± 0.11	0.60 ± 0.19	13.1
REF (3)	for $\lvert\Delta p_T\rvert<\lvert\Delta p_{\parallel}\rvert$	0.44 ± 0.05	0.71 ± 0.12	20.3

*) After C_λ correction

+) The quoted errors are given by the fit where the parameters were found to be correlated.

Figure Captions

Fig. 1 The effective correction factor as a function of $\tilde{M}^2$ for (π^-,π^-) and (π^+,π^+) combinations.

Fig. 2 The ratios of the $\tilde{M}^2$ distributions for like-sign pions and the three different reference samples which do not contain the Bose-Einstein interference.

a) the ratios from the data. The parameters of the fitted lines are given in the text,

b) the ratios expected from the Lund model [19],

c) the ratios from the data divided by the corresponding ratios from the Lund model. Results of the fits are given in table 1.

Fig. 3 The relative resonance contribution in the $\tilde{M}^2$ distribution of like-sign pions and of (π^+,π^-) combinations as predicted by the Lund model. The uppermost line shows the prediction for the LIKE/(π^+,π^-)ratio for pions which do not originate from η, η', ρ^o and ω^o decays. The vertical arrows show the position of the $\tilde{M}^2$ value for ρ^o and ω decays into $\pi^+\pi^-$. The horizontal regions show the contribution from the decays into 3π.

Fig. 4. The ratio of LIKE/REF (3) from the data divided by the same ratio expected from the Lund model, as a function of $\tilde{M}^2$, for pairs of pions whose energies in the hadronic CMS are different by less than 0.2 GeV. The results of the fit are shown by the solid line for which the parameters are given in table 1. The broken line shows the results of the fit to the same ratio for all ΔE values (see also table 1).

Fig. 5 The ratio of LIKE/REF (3) from the data divided by the same ratio expected from the Lund model, as a function of $\tilde{M}^2$ for pion pairs from the shaded regions. In $(\Delta p_{\parallel},\Delta p_T)$ plane; a) $|\Delta p_T|>|\Delta p_{\parallel}|$, b) $|\Delta p_T|<\Delta p_{\parallel}|$. The results of the fits are shown by the solid lines for which the parameters are given in table 1. The broken line shows the results of the fit to the same ratio for all pion pairs (see also table 1).

Fig. 6 The ratio of LIKE/REF (3) from the data divided by the same ratio expected from the Lund model for pion pairs from the shaded regions in $(\Delta p_{\parallel}, \Delta p_T)$ plane; the black points - as a function of Δp_T^2 for $|\Delta p_{\parallel}^2| < 0.04$ GeV^2, the white points - as a function of $\Delta p_{\parallel}^2$ for $|\Delta p_T^2| < 0.024$GeV^2. The broken line shows the results of the fit to the same ratio for all pion pairs.

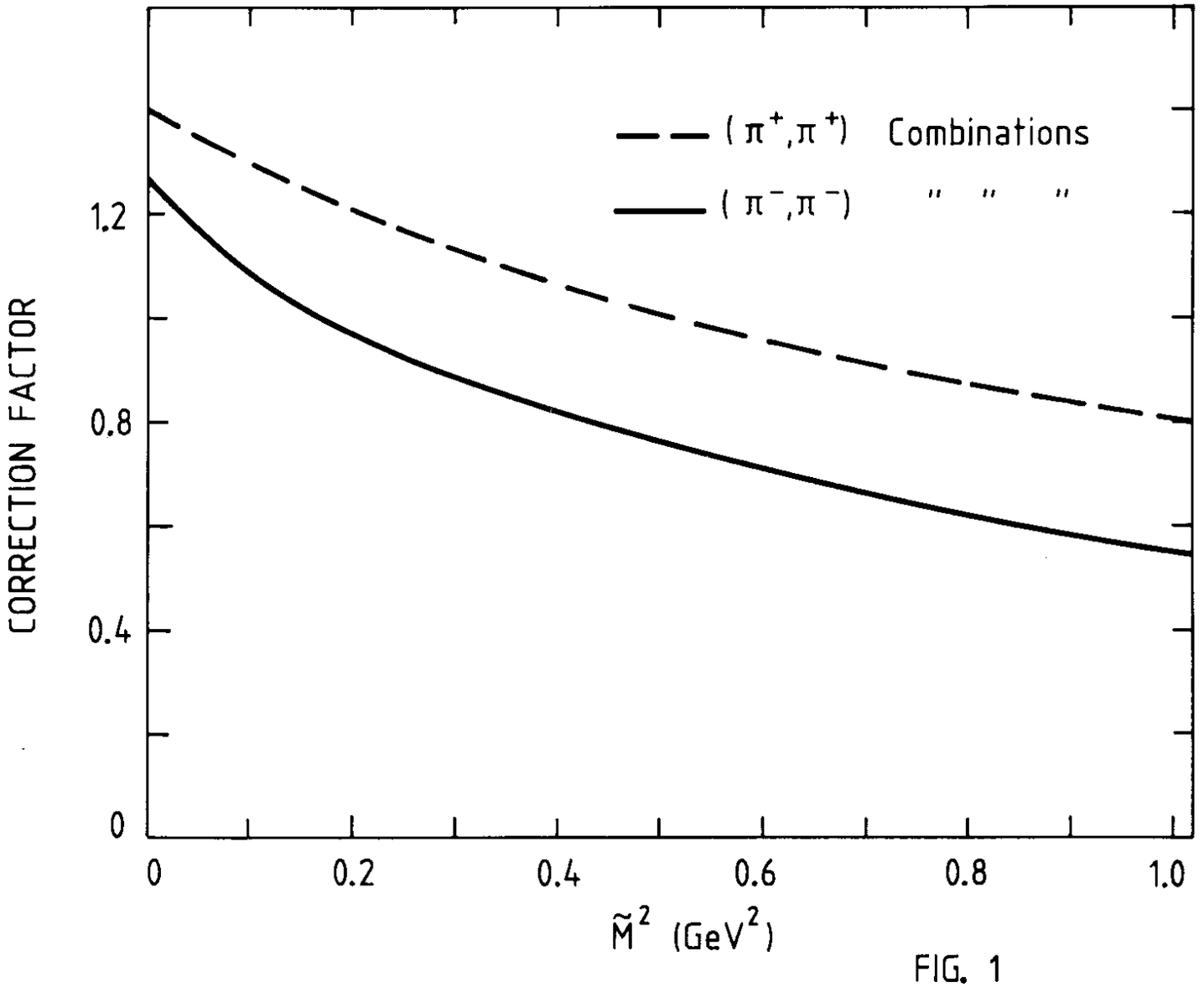
(π+,π+) Combinations
(π−,π−) " " "
CORRECTION FACTOR
1.2
0.8
0.4
0
0
0.2
0.4
0.6
0.8
1.0
M̃² (GeV²)

FIG. 1

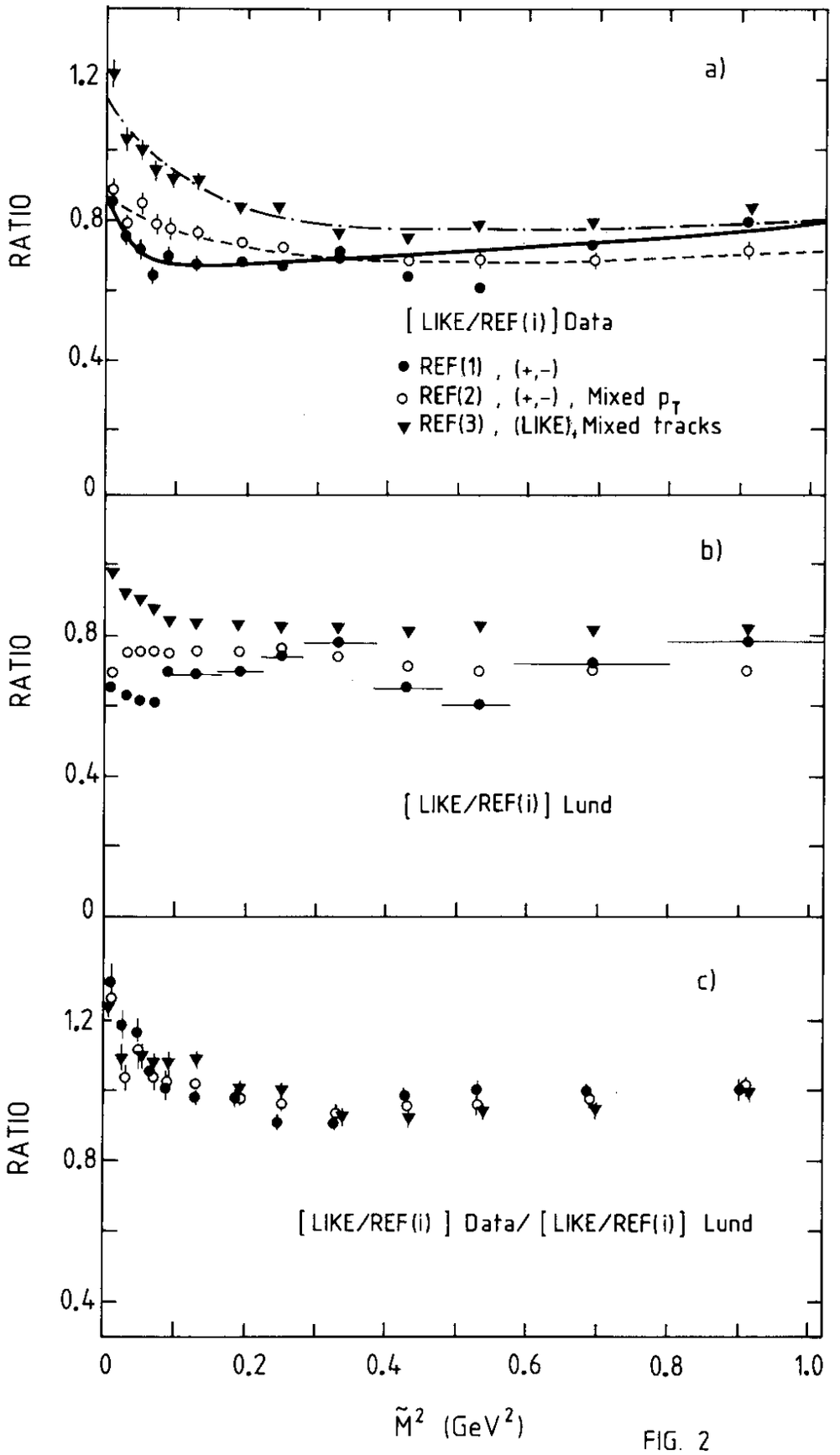
a)
b)
c)
RATIO
RATIO
RATIO
1.2
0.8
0.4
0
1.2
0.8
0.4
0
0.8
0.4
[LIKE/REF(i)] Data
● REF(1) , (+,-)
○ REF(2) , (+,-) , Mixed p_T
▼ REF(3) , (LIKE)+ Mixed tracks
[LIKE/REF(i)] Lund
[LIKE/REF(i)] Data/ [LIKE/REF(i)] Lund
0
0.2
0.4
0.6
0.8
1.0
$\tilde{M}^2$ (GeV^2)

FIG. 2

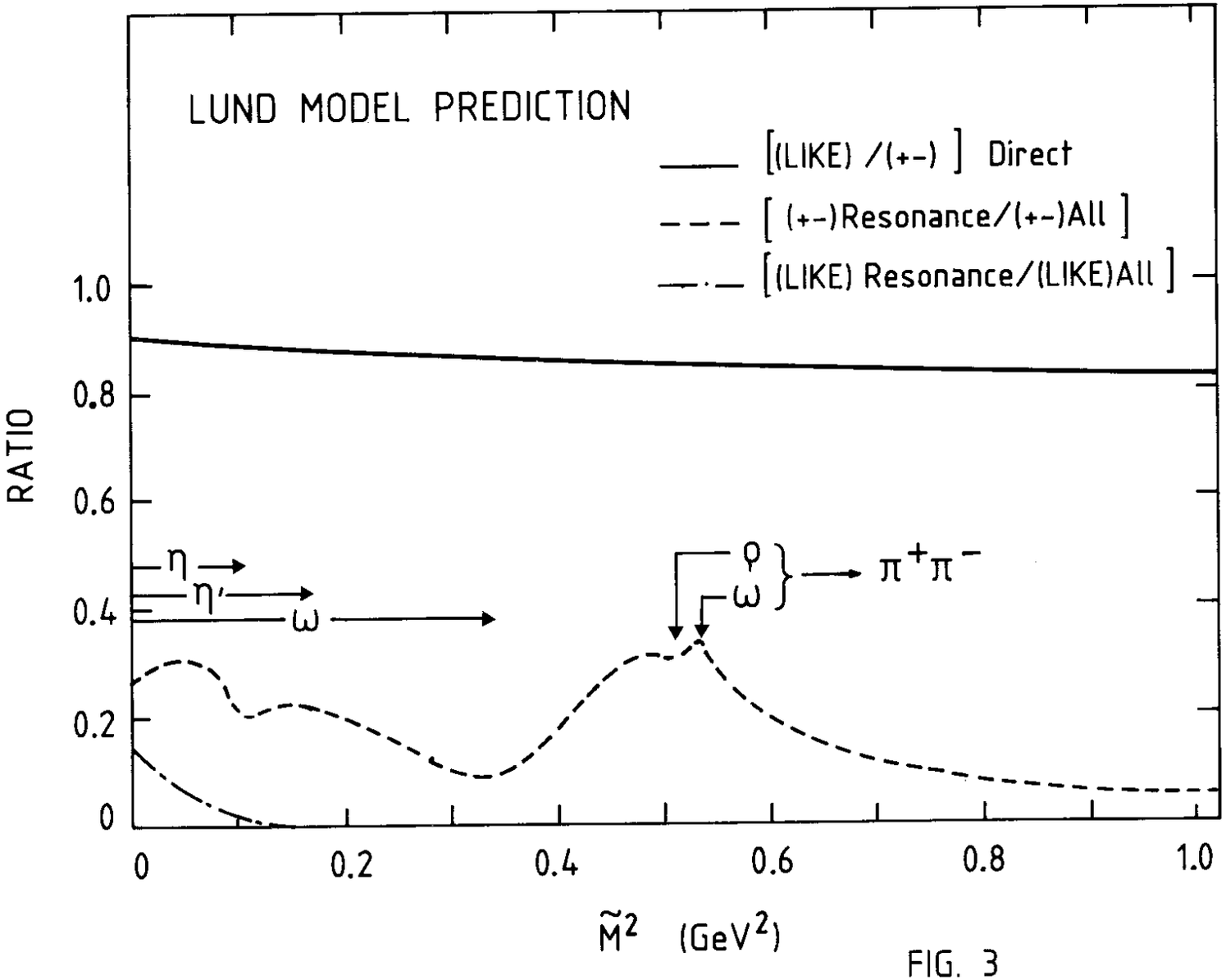
LUND MODEL PREDICTION
[(LIKE) /(+-)] Direct
[(+-)Resonance/(+-)All]
[(LIKE) Resonance/(LIKE)All]
RATIO
1.0
0.8
0.6
0.4
0.2
0
η
η'
ω
ρ
ω
π+π−
0
0.2
0.4
0.6
0.8
1.0
M̃2 (GeV2)

FIG. 3

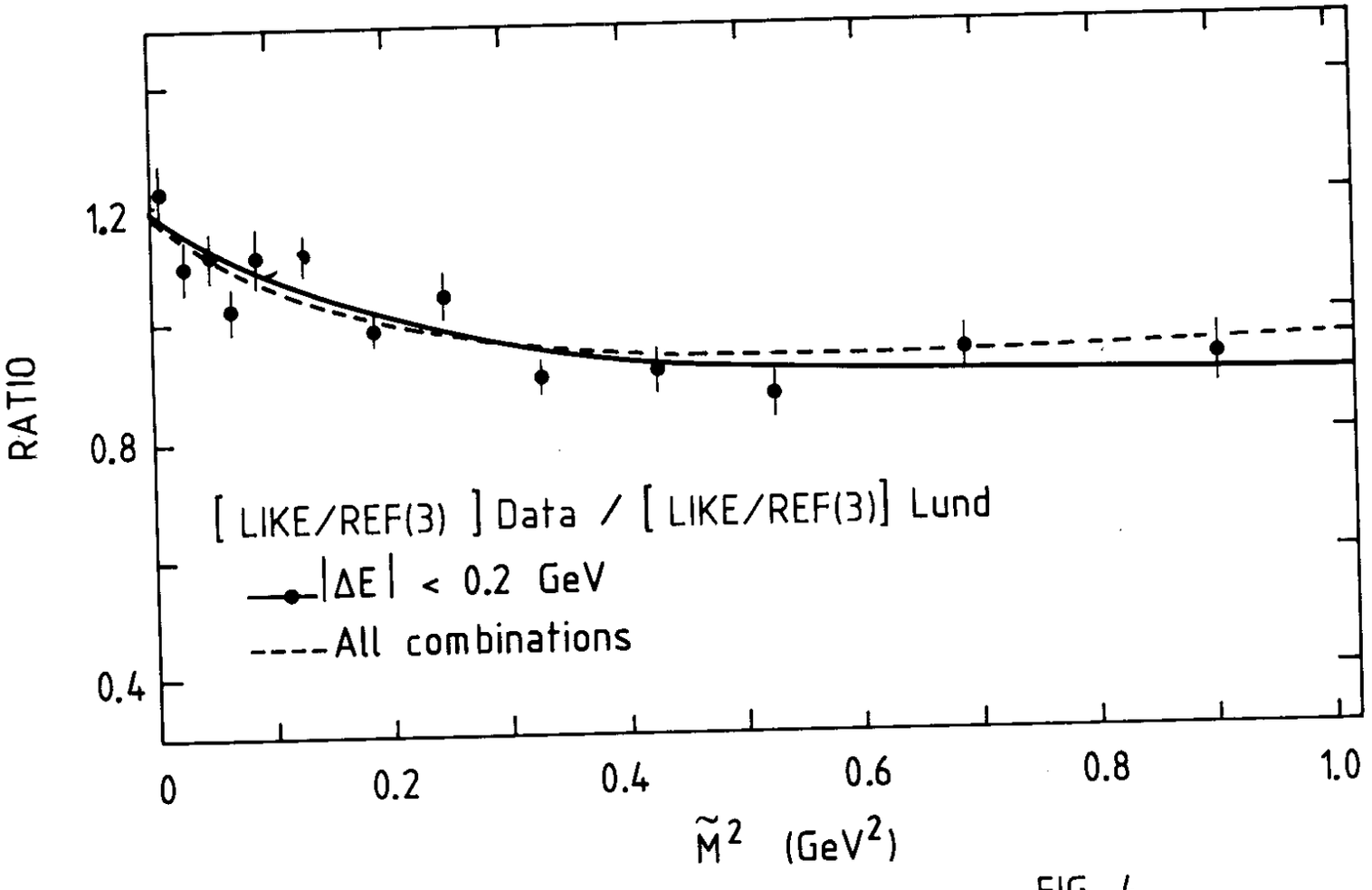
RATIO
1.2
0.8
0.4
[LIKE/REF(3)] Data / [LIKE/REF(3)] Lund
|ΔE| < 0.2 GeV
All combinations
0
0.2
0.4
0.6
0.8
1.0
$\tilde{M}^2$ (GeV^2)

FIG. 4

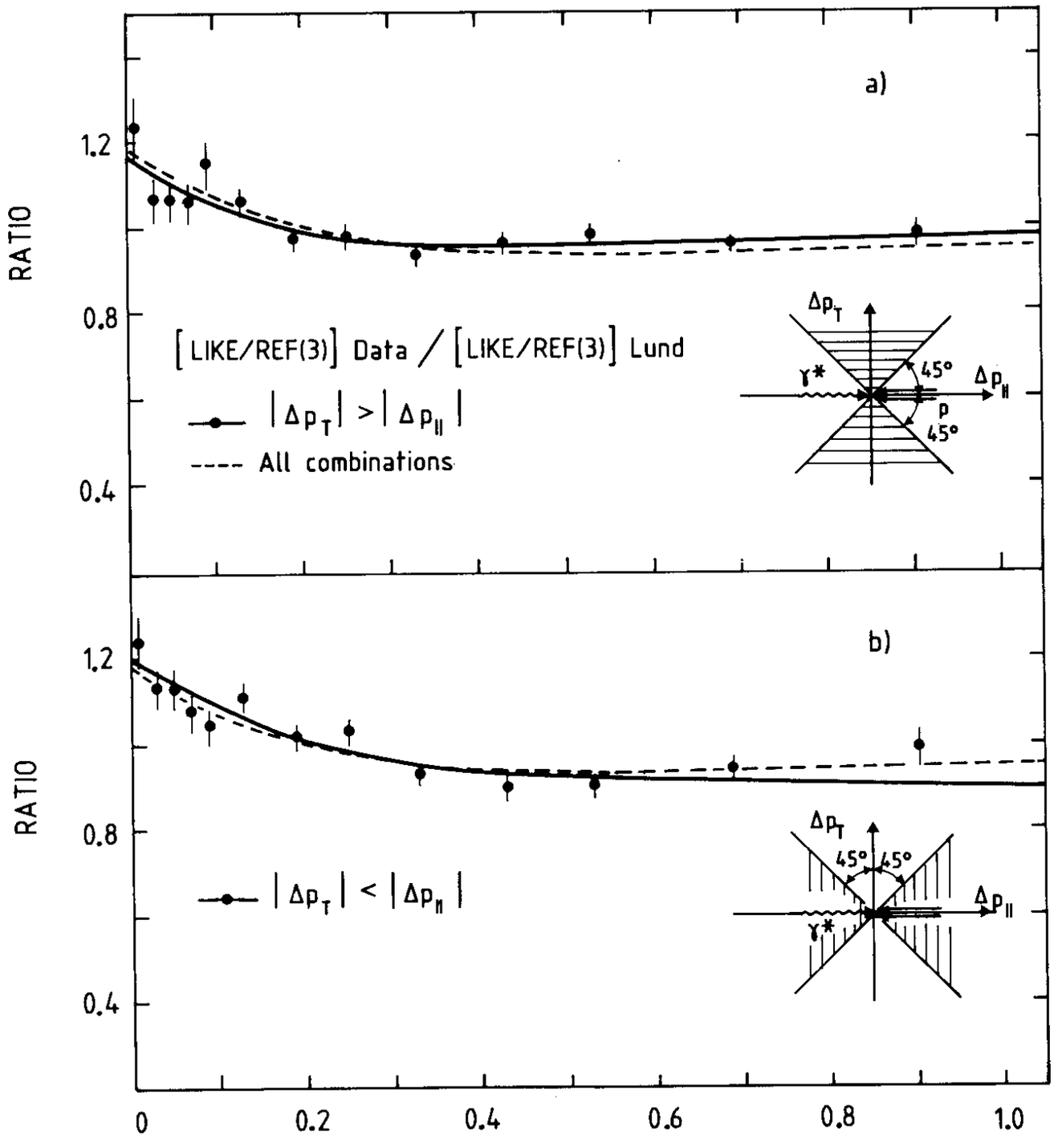
a)
b)
RATIO
RATIO
1.2
0.8
0.4
[LIKE/REF(3)] Data / [LIKE/REF(3)] Lund
$|\Delta p_T| > |\Delta p_{II}|$
All combinations
$|\Delta p_T| < |\Delta p_{II}|$
Δp_T
Δp_{II}
γ^*
45°
p
0
0.2
0.4
0.6
0.8
1.0
$\tilde{M}^2$ (GeV^2)

FIG. 5

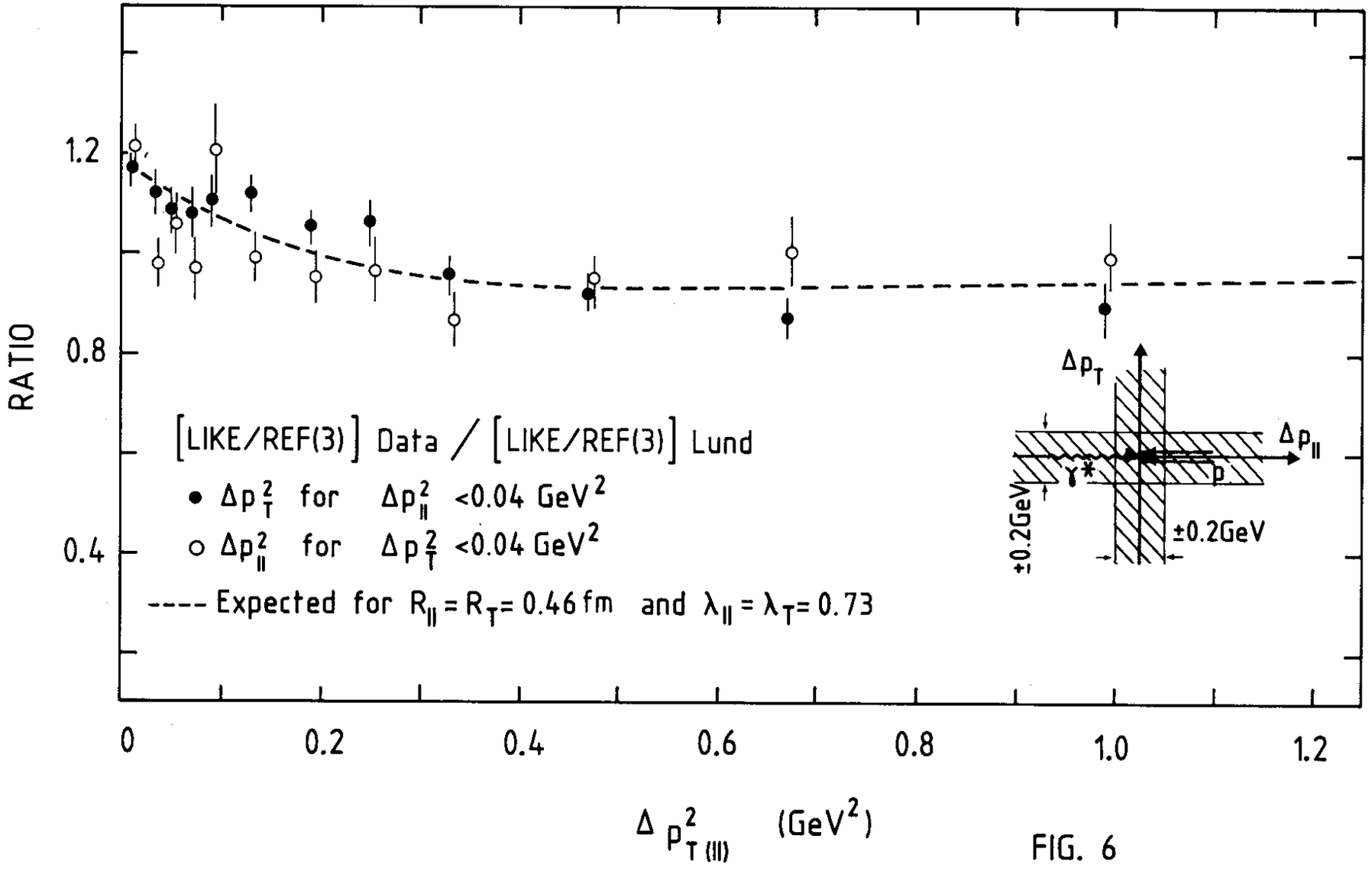
RATIO
1.2
0.8
0.4
0
0.2
0.4
0.6
0.8
1.0
1.2
[LIKE/REF(3)] Data / [LIKE/REF(3)] Lund
• Δp_T^2 for Δp_{II}^2 <0.04 GeV^2
○ Δp_{II}^2 for Δp_T^2 <0.04 GeV^2
---- Expected for $R_{II} = R_T = 0.46$ fm and $\lambda_{II} = \lambda_T = 0.73$
Δp_T
Δp_{II}
γ*
p
±0.2GeV
±0.2GeV
$\Delta p_{T(II)}^2$ (GeV^2)

FIG. 6